DOI: 10.1002/ejic.200700757

Orientation and Arrangement of Octaruthenium Supramolecules with Alkyl Chains on Graphite

Dong-Lin Shieh,[a] Yi-Shiue Lin,[a] Kom-Bei Shiu,[a] and Jong-Liang Lin*[a]

Keywords: Supramolecular chemistry / Scanning tunneling microscopy / Ruthenium

The self-assemblies of octaruthenium grid-type supramolecules, $\{[Ru_2(CO)_4(NH_2C_{16}H_{33})_2](\mu\text{-}O_2CCO_2)\}_4$, on highly oriented pyrolytic graphite (HOPG) in air and in 1-phenyloctane were studied by scanning tunneling microscopy (STM). The surface supramolecules are arranged into rows in which the metal cores are linearly packed and the alkyl chains are parallel to the surface. With the aid of theoretical calculations in the framework of density functional theory, the electronic origin of the tunneling in the measured STM images is discussed.

Introduction

Nanoscience and nanotechnology have great potential for making a significant impact on our society. The design and fabrication of nanoscaled structures with functional properties have attracted considerable attention recently. A host of devices can be miniaturized by shrinking them in size (top-down approach). An alternative is a bottom-up approach based on assembly of building units at the molecular level. Self-organization and self-assembly are a well-established phenomenon and are critically important in living organisms as well as chemistry and material science.[1] Supramolecules formed through coordination chemistry exhibit versatile structures (square, triangle, cage, etc.) and ample metal-based or ligand-based functionality.[2,3] The incorporated electronic, magnetic, photochemical, photophysical, redox, and/or catalytic properties can lead to applications in molecular recognition, electrochemical sensing, information storage, catalysis, and so on. In addition, the well-defined cavities of the supramolecules create the possibilities of host–guest and inclusion chemistries.[4] As particle or device size diminishes, the ratio of surface area to volume increases and surface properties play a crucial role. Recently, ordered assemblies of supramolecules with transition-metal cyclic structures on surfaces were reported, such as grid-type Co, Zn, and Fe complexes on HOPG,[5] octaruthenium and tetraruthenium complexes on HOPG,[6] Pt complexes with shapes of rectangle, square, and cage on Au(111),[7] and square Pt complexes on chloride-covered Cu(100).[8] From a technological point of view, several key parameters need to be precisely controlled for these complexes, including physical and chemical properties, surface distribution, and molecular orientation of adsorbates.[4] A monolayer film structure is a combined result of the interactions between adsorbed molecules and the substrate and between adsorbed molecules themselves, which can be controlled by hydrogen bonding, dipole–dipole coupling, steric effects, and so on. Cu^{II} salicyclic aldehyde complexes and aldimine derivative complexes show different adsorption layer lattices on HOPG,[9] that is, a film structure is modified by ligand substitution. Ligand substitution or only introduction of specific functional groups at given positions in the ligand moieties opens a pathway to control not only two-dimensional film structure but also the molecular orientation in the films.[5a] Recently, we reported that $\{[Ru_2(CO)_4(PMe_3)_2](\mu\text{-}O_2CCO_2)\}_4$, an octaruthenium supramolecule with a square shape (Figure 1, structure **1**), forms two kinds of two-dimensional, well-ordered assemblies on HOPG in air. One of the assemblies is composed of supramolecules containing Ru–Ru bonds perpendicular to the surface and the PMe_3 groups as outermost parts. In the other assembly, the supramolecules adopt an orientation with the Ru–Ru bonds parallel to the surface and the CO groups as outermost parts. The identification of the layer structure was based on the direct comparison of the dimensions of the octaruthenium supramolecule with the size of the bright lobes observed in the STM images. In the present study, we demonstrate the formation of a two-dimensional assembly of $\{[Ru_2(CO)_4(NH_2(CH_2)_{15}CH_3)_2](\mu\text{-}O_2CCO_2)\}_4$ on HOPG (Figure 1, structure **2**), in which the supramolecules are arranged in rows and the Ru–Ru bonds are parallel to the substrate surface. The possible tunneling origin for the observed images of the octaruthenium molecules is discussed with the aid of density functional theory calculations.

[a] Department of Chemistry, National Cheng Kung University, 1, Ta Hsueh Road, Tainan, Taiwan 701, Republic of China
Fax: +886-6-2740552
E-mail: jonglin@mail.ncku.edu.tw
Supporting information for this article is available on the WWW under http://www.eurjic.org or from the author.

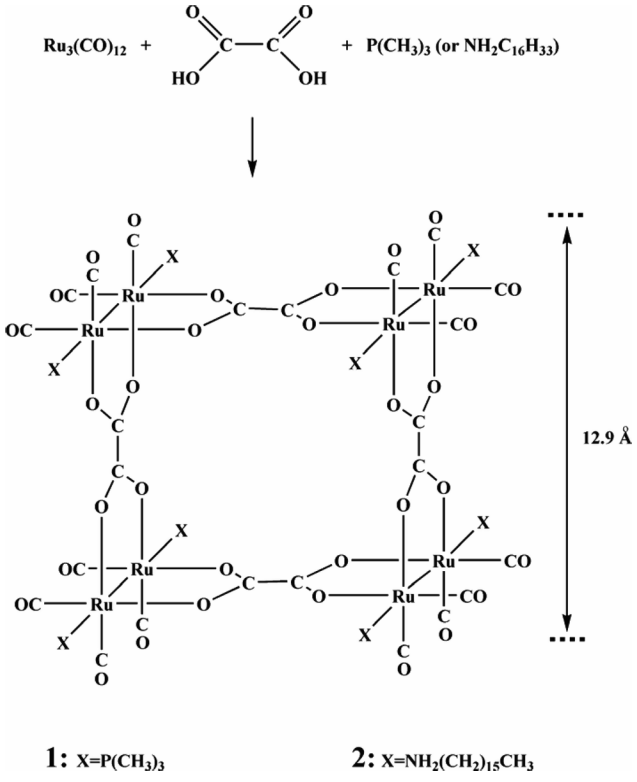

Figure 1. Formation of the grid-type octaruthenium complexes.

Results and Discussion

Figure 2a presents a 15.0×15.0 nm^2 STM image of **2** on HOPG, assembled in CH_2Cl_2 and measured in air with a positive sample bias of 0.25 V in constant current mode (0.098 nA). This image shows a structure constituted by parallel rows. The width of each row is approximately 49.0 Å, with a linear bright region in the center area. The row width is close to the length (48 Å) of **2** calculated from one CH_3 end group to the other one on the opposite side across the metal cores on the basis of the theoretically optimized structure of **2** with zig–zag hydrocarbon chains. Figure 2b compares the *I–V* curve measured at the bright area in Figure 2a to the typical *I–V* curve of the pure HOPG plane. In the former case, the flat *I–V* feature about the zero bias voltage shows the presence of a bandgap. The measurements of the tunneling current at every bias were made three times and averaged to improve the signal-to-noise ratio. In some areas of **2**-covered HOPG, edges of islands formed by the ordered arrangement of the supramolecules can be observed. Figure 3a is a 600×600 nm^2 STM image, measured with a sample bias of –0.07 V and a tunneling current of 0.049 nA in air; it shows a step separating two terraces. On the basis of the tunneling image and the *I–V* spectrum measured around point A in the lower area (not shown), the dark terrace is attributed to a clean graphite surface. The row-like feature of Figure 2a is also observed in the high-resolution STM images taken in the bright terrace of Figure 3a, as shown in Figure S1 (Supporting Information). The line profile across the step (from point A to B) shows that the height difference between the two terraces is approximately 17 Å (Figure 3b), which is close to the height of the molecule, ca. 15.9 Å [sum of the oxygen nucleus-to-nucleus distance (12.9 Å, as indicated in Figure 1) and the van der Waals radii of two oxygen atoms (ca. 3 Å)]. These geometric similarities, the row width corresponding to the molecular length and the island height corresponding to the molecular height, indicate that the adsorbed supramolecules adopt an orientation with their long hydrocarbon chains and Ru–Ru bonds parallel to the surface. For an adsorbed molecule of **2** with this orientation, there are four coordinated CO molecules in contact with the surface.

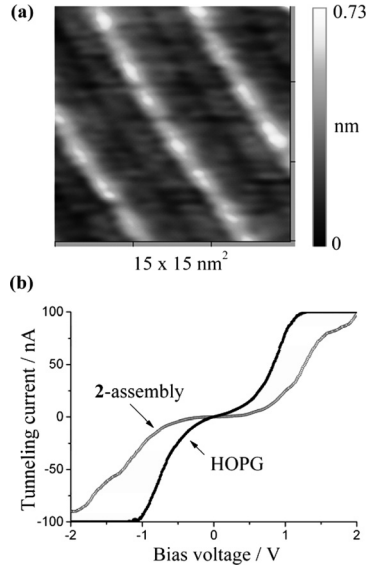

Figure 2. (a) STM image measured with a positive sample bias voltage of 0.25 V and a tunneling current of 0.098 nA in air of the assembly of **2** on HOPG. The width of the rows corresponds to the length of the molecule; (b) comparison of the *I–V* curves of clean and **2**-covered HOPG surfaces.

Because the formation of the layer structure of **2** on HOPG must depend on the interactions between **2** and the HOPG surface as well as on the interactions between molecules of **2**, a model compound, $\{[Ru_2(CO)_4(NH_3)(NH_2\text{-}C_8H_{17})](\mu\text{-}O_2CCO_2)\}_4$, on HOPG was calculated to address the bonding nature of **2**. In these calculations, the HOPG surface is represented by a sheet of carbon atoms fixed at the graphite lattice positions, with the edge carbon atoms coordinately saturated with H atoms. The total atom number (500 atoms) was confined by the software package in computation; therefore, only the model compound was studied instead of **2**. For the two adsorption systems of Figure 4a, b in which the adsorbed molecules have a 10° directional difference, the energy discrepancy is only 3 kcal mol^{-1}. This small difference in energy can be attributed to the weak van der Waals interaction between the molecule and the surface, which is not strongly dependent on the adsorption sites. The optimized 2.9 Å distance between the graphite surface and the O atom of the terminal CO (Figure 4a) is consistent with the sum of the van der Walls radii of C and O.

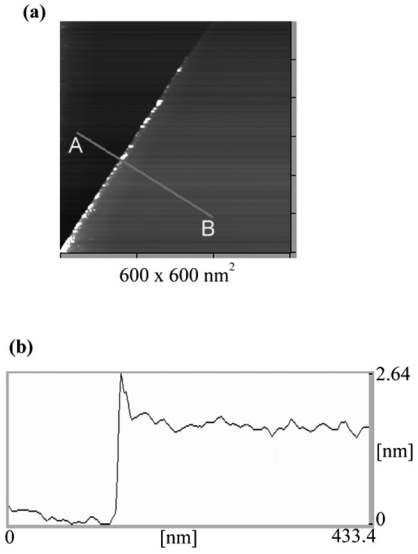

Figure 3. (a) A 600×600 nm^2 STM image measured in air with a sample bias voltage of –0.07 V and a tunneling current of 0.049 nA of a step separating a bright terrace representing a **2**-covered area and a dark terrace representing an uncovered area of HOPG; (b) the line profile from A to B shows that the height between the two terraces is ca. 17 Å.

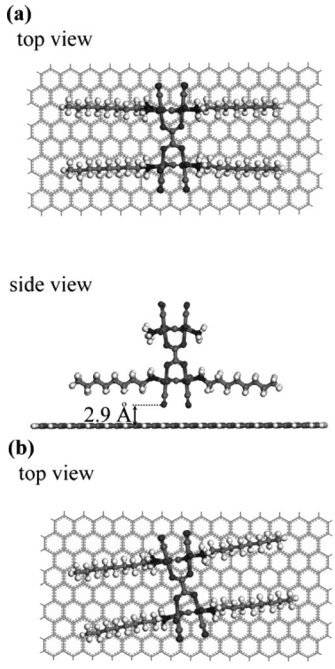

Figure 4. Optimized adsorption structures of a $\{[Ru_2(CO)_4(NH_3)(NH_2C_8H_{17})][\mu\text{-}O_2CCO_2]\}_4$ model compound in different directions (10° difference); structure (b) has an energy that is only 3 kcal mol^{-1} higher.

To check the effect of the presence of solvent molecules on the adsorption structure and 2D array of **2** on HOPG, the assembly of **2** on HOPG was assembled and probed by STM in 1-phenyloctane. In a recent STM study of hexadehydrotribenzo[12]annulene derivatives (DBA) on HOPG, it was found that the structure of the DBA networks on HOPG is dramatically influenced by the presence of different solvent molecules.[10] The STM image of the ordered layer structure of **2** on HOPG measured in 1-phenyloctane with a +1.9 V sample bias voltage and a tunneling current of 0.049 nA is presented in Figure 5a. The molecules of **2** are packed into rows with a width of ca. 46.5 Å, similar to that observed in air. Figure 5b is a magnified image of the center region of Figure 5a, with a superimposed structure of **2** to show the matched length.

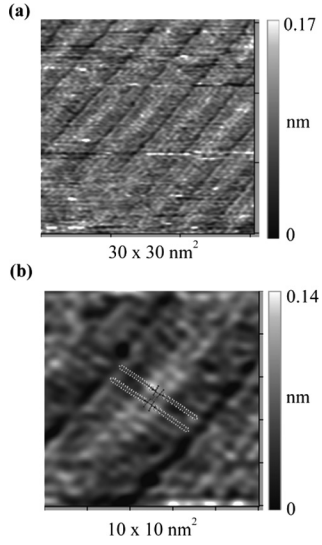

Figure 5. (a) A 30 nm × 30 nm STM image measured with a sample bias voltage of 1.9 V and a tunneling current of 0.049 nA in 1-phenyloctane of the assembly of **2** on HOPG; (b) magnified graph of the center region of (a) with a superimposed molecule of **2**.

To further address the origin of the tunneling, the molecular orbitals from the HOMO to HOMO-10 and from the LUMO to LUMO+9 of **2** were calculated in the framework of density functional theory (LDA-PWC). HOMO-*n* denotes the orbital below the HOMO by n energy levels; LUMO+*n* denotes the orbital above the LUMO by n energy levels. The wavefunctions from the HOMO to HOMO-3 of **2** and their relative energies are shown in Figure 6. The orbitals from the HOMO-4 to HOMO-10 are displayed in Figure S2 (Supporting Information). The orbitals from the HOMO to HOMO-3 mainly comprise Ru $4d_{z^2}$, N $2p_z$, and C $2p_z$ of the CO group and O $2p_z$ of the CO and O_2CCO_2 groups. The orbitals from the HOMO-4 to HOMO-7 contain the components of Ru 4d, N 2p, and O 2p of the CO and O_2CCO_2 groups. Ru 4d and O 2p of the CO and O_2CCO_2 groups contribute to the orbitals from HOMO-8 to HOMO-10. Figure 7 and Figure S3 (Supporting Information) show that the predominant contributions of the orbitals from the LUMO to LUMO+4 are C 2p and O 2p of the bridging O_2CCO_2 group. The orbitals from the LUMO+5 to LUMO+9 mainly consist of Ru 4d, C 2p, and O 2p of the terminal CO group. Our DFT calculations (LDA-PWC and GGA-PBE) show that the HOMO–LUMO gap of **2** is ca. 1.2 V. The self-assembled layer of **2** on HOPG in air was imaged at a small bias voltage of +0.25 V (Figure 1a). Different mechanisms were proposed for STM images of adsorbed molecules measured at low

bias voltages, in the gap between the HOMO and LUMO states, including work function modulation, resonant tunneling, and weak mixing of states of the molecule and substrate through molecule–substrate interaction.[11] In the case of the STM image of **2** assembled and measured in 1-phenyloctane, a +1.9 V sample bias was used. With an assigned HOMO–LUMO energy gap of 1.2 V and the assumption that the substrate Fermi level is located at the midpoint in the gap, the calculated energy levels from the LUMO to LUMO+9 are all below the Fermi level at a positive bias of 1.9 V, that is, these states become accessible for electron tunneling from HOPG to the molecules.

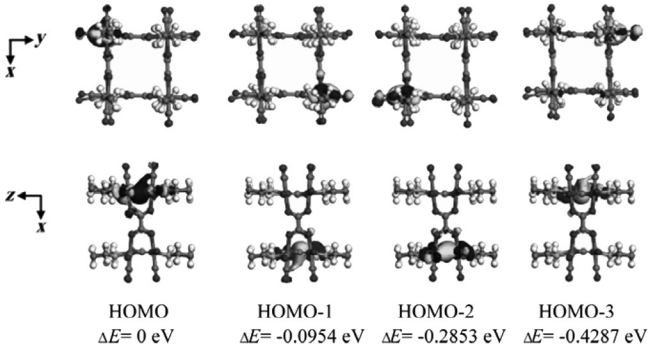

Figure 6. Individual molecular orbitals of **2** from the HOMO to HOMO-3 and their relative energies. $NH_2C_2H_5$ is used to replace $NH_2C_{16}H_{33}$ to save space.

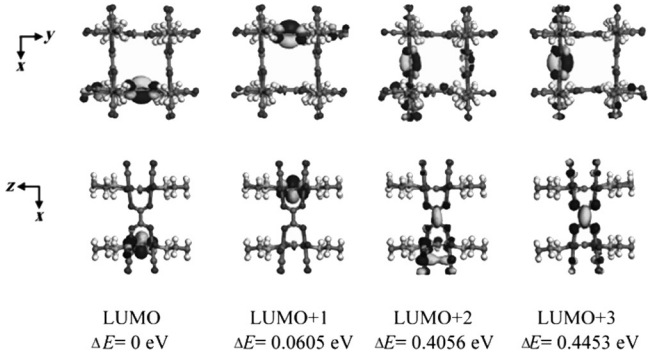

Figure 7. Individual molecular orbitals of **2** from the LUMO to LUMO+3 and their relative energies. $NH_2C_2H_5$ is used to replace $NH_2C_{16}H_{33}$ to save space.

Conclusions

Grid-type octaruthenium complex **2** consisting of CO and $NH_2C_{16}H_{33}$ terminal ligands and a O_2CCO_2 bridging ligand was designed, synthesized, and studied with STM. Molecules of **2** on HOPG form an ordered assembly in which the molecules are arranged into rows, and they adopt an orientation with their Ru–Ru bonds and hydrocarbon chains parallel to the surface.

Experimental Section

Synthesis of $[Ru_2(CO)_4(NH_2C_{16}H_{33})_2](\mu\text{-}O_2CCO_2)_4$: Freshly prepared $[Ru_3(CO)_{12}]$, oxalic acid·$2H_2O$, and THF were added in a pressure Schlenk tube. The mixture was heated to 120 °C while magnetically stirred for 6 h. To avoid the back-reaction, the gases evolved were drawn off from time to time. *n*-Hexadecylamine was then added. The solution was stirred for 2 h more, and then the solvents were removed under vacuum to afford a solid residue. Recrystallization from CH_2Cl_2/MeOH gave $[Ru_2(CO)_4(NH_2C_{16}H_{33})_2](\mu\text{-}O_2CCO_2)_4$. Yield: 83%. ^1H NMR (300 MHz, CD_2Cl_2): δ = 0.86 (t, J = 6.4 Hz, 24 H, terminal CH_3), 1.54 (m, 16 H, CH_2CH_3), 2.32 (s, NH_2), 2.91 (t, J = 7.1 Hz, 16 H, CH_2NH_2), 1.25 (m, 208 H, $104 \times CH_2$). IR (CH_2Cl_2): $\tilde{\nu}$ = 1591 (CO), 1979 (CO), 2030 (CO) cm^{-1}. $C_{152}H_{280}N_8O_{32}Ru_8$ (3540.47): calcd. C 51.6, H 8.0, N 3.2; found C 51.4, H 8.0, N 3.2.

$[Ru_2(CO)_4(NH_2C_{16}H_{33})_2](\mu\text{-}O_2CCO_2)_4$ Film Preparation for STM Investigation: The 2D layer structure of $[Ru_2(CO)_4(NH_2C_{16}H_{33})_2](\mu\text{-}O_2CCO_2)_4$ on HOPG was investigated in air and in 1-phenyloctane. The film formation procedures for these two STM studies were different. In the former case, a drop of $[Ru_2(CO)_4(NH_2C_{16}H_{33})_2](\mu\text{-}O_2CCO_2)_4$ in CH_2Cl_2 (0.01 M) was deposited on a freshly cleaved surface of HOPG (ZYB quality), which was placed in the middle of a glass container with a small amount of CH_2Cl_2 left on the bottom, and then the container was sealed immediately. After 6 h, the HOPG was taken out of the container and the CH_2Cl_2 was allowed to vaporize before STM images were recorded. It was found that **2** with the long alkyl chains $[-(CH_2)_{15}CH_3]$ needed much more time, relative to molecules of **1** reported previously, to pack into an ordered assembly by diffusion and adjustment of their relative positions in the interface of the solvent (CH_2Cl_2) and HOPG. In the case of **2** in 1-phenyloctane, a drop of 1-phenyloctane solution saturated with $[Ru_2(CO)_4(NH_2C_{16}H_{33})_2](\mu\text{-}O_2CCO_2)_4$ was placed on a freshly cleaved HOPG surface, which allowed the formation of an assembly of **2**. After 6 h, the surface was scanned by STM. Electrochemically etched W tips were used for the STM studies (Seiko Instruments, SPA 400) at constant current mode. All the STM images were collected with 256×256 data points.

Molecular Orbital Calculations: The optimized molecular structure as well as the orbitals and energies of $[Ru_2(CO)_4(NH_2C_{16}H_{33})_2](\mu\text{-}O_2CCO_2)_4$ were calculated in the framework of density functional theory by using the DMol^3 package, in which the Perdew–Wang local exchange and correlation function (LDA-PWC) and double-numerical basis set were employed. The calculations were spin-unrestricted and did not include a relativistic effect for the core electrons. In addition, another method, the generalized gradient approximation of Perdew, Burke, and Ernzerhof to the exchange and correlation functional (GGA-PBE), was also employed to calculate the supramolecular orbitals and their corresponding energies. A consistent HOMO–LUMO energy gap was obtained with both methods.

Supporting Information (see footnote on the first page of this article): Additional STM image and the HOMO- and LUMO-related orbitals of **2**.

Acknowledgments

This research was financially supported by the National Science Council of the Republic of China (NSC 95-2113-M-006-017-MY2).

[1] a) J. U. Lane, J. L. Atwood, J. E. D. Davies, D. D. MacNicol, F. Vögtle (Eds.), *Comprehensive Supramolecular Chemistry*, Pergamon, Oxford, **1996**, vol. 9; b) G. F. Swiegers, T. J. Malefetse, *Chem. Rev.* **2000**, *100*, 3483–3538; c) G. M. Whitesides, M. Boncheva, *Proc. Natl. Acad. Sci. USA* **2002**, *99*, 4769–4774.

[2] a) N. L. S. Yue, M. C. Jennings, R. J. Puddephatt, *Inorg. Chem.* **2005**, *44*, 1125–1131; b) M. P. Martin-Redondo, L. Scoles, B. T. Sterenberg, K. A. Udachin, A. J. Carty, *J. Am. Chem. Soc.* **2005**, *127*, 5038–5039; c) F. A. Cotton, C. A. Murillo, X. Wang, R. Yu, *Inorg. Chem.* **2004**, *43*, 8394–8403; d) D. C. Caskey, R. K. Shoemaker, J. Michl, *Org. Lett.* **2004**, *6*, 2093–2096; e) J. Forniés, J. Gómez, E. Lalinde, M. T. Moreno, *Chem. Eur. J.* **2004**, *10*, 888–898; f) S. J. Lee, J. S. Kim, W. Lin, *Inorg. Chem.* **2004**, *43*, 6579–6588; g) K. Kumazawa, Y. Yamanoi, M. Yoshizawa, T. Kusukawa, M. Fujita, *Angew. Chem. Int. Ed.* **2004**, *43*, 5936–5940; h) P. Angaridis, J. F. Berry, F. A. Cotton, C. A. Murillo, X. Wang, *J. Am. Chem. Soc.* **2003**, *125*, 10327–10334; i) Y. K. Kryschenko, S. R. Seidel, A. M. Arif, P. J. Stang, *J. Am. Chem. Soc.* **2003**, *125*, 5193–5198; j) Z. Qin, M. C. Jennings, R. J. Puddephatt, *Inorg. Chem.* **2002**, *41*, 3967–3974.

[3] a) S. Alvarez, *Dalton Trans.* **2005**, 2209–2233; b) Y. X. Ke, D. J. Collins, H. C. Zhou, *Inorg. Chem.* **2005**, *44*, 4154–4156; c) M. Fujita, M. Tominaga, A. Hori, B. Therrien, *Acc. Chem. Res.* **2005**, *38*, 369–378; d) D. L. Reger, R. F. Semeniuc, M. D. Smith, *Inorg. Chem.* **2003**, *42*, 8137–8139; e) U. Radhakrishnan, M. Schweiger, P. J. Stang, *Org. Lett.* **2001**, *3*, 3141–3143; f) C. J. Kuehl, T. Yamamoto, S. R. Seidel, P. J. Stang, *Org. Lett.* **2002**, *4*, 913–915; g) B. J. Holliday, C. A. Mirkin, *Angew. Chem. Int. Ed.* **2001**, *40*, 2022–2043.

[4] B. J. Holliday, C. A. Mirkin, *Angew. Chem. Int. Ed.* **2001**, *40*, 2022–2043.

[5] a) A. Semnov, J. P. Spatz, M. Möller, J.-M. Lehn, B. Sell, D. Schubert, C. H. Weidle, U. S. Schubert, *Angew. Chem. Int. Ed.* **1999**, *38*, 2547–2550; b) U. Ziener, J.-L. Lehn, A. Mourran, M. Möller, *Chem. Eur. J.* **2002**, *8*, 951–957; c) M. S. Alam, S. Strömsdörfer, V. Dremov, P. Müller, J. Kortus, M. Ruben, J.-M. Lehn, *Angew. Chem. Int. Ed.* **2005**, *44*, 7869–7900; d) A. Mourran, U. Ziener, M. Möller, E. Breuning, M. Ohkita, J.-M. Lehn, *Eur. J. Inorg. Chem.* **2005**, 2641–2647; e) M. Ruben, J. Rojo, F. J. Romero-Salguero, L. H. Uppadine, J.-M. Lehn, *Angew. Chem. Int. Ed.* **2004**, *43*, 3644–3662.

[6] D.-L. Shieh, K.-B. Shiu, J.-L. Lin, *Eur. J. Inorg. Chem.* **2004**, 2223–2227.

[7] Q.-H. Yuan, L.-J. Wan, H. Jude, P. T. Stang, *J. Am. Chem. Soc.* **2005**, *127*, 16279–16286.

[8] C. Safarowsky, L. Merz, A. Rang, P. Broekmann, B. A. Hermann, C. A. Schalley, *Angew. Chem. Int. Ed.* **2004**, *43*, 1291–1294.

[9] P. Zell, F. Mögele, U. Ziener, B. Rieger, *Chem. Commun.* **2005**, 1294–1296.

[10] K. Tahara, S. Furukawa, H. Uji-i, T. Uchino, T. Ichikawa, J. Zhang, W. Mamdouh, M. Sonoda, F. C. De Schryver, S. De Feyter, Y. Tobe, *J. Am. Chem. Soc.* **2006**, *128*, 16613–16625.

[11] a) J. K. Spong, H. A. Mizes, L. J. LaComb Jr, M. M. Dovek, J. E. Frommer, J. S. Foster, *Nature* **1990**, *338*, 137–139; b) W. Mizutani, M. Shigeno, M. Ono, K. Kajimura, *Appl. Phys. Lett.* **1990**, *56*, 1974–1976; c) Z. Klusek, W. Kolowski, *J. Electron Spectrosc. Relat. Phenom.* **2000**, *107*, 63–72; d) A. J. Fisher, P. E. Blöchl, *Phys. Rev. Lett.* **1993**, *70*, 3263–3266.

Received: July 18, 2007
Published Online: October 24, 2007

